

Fabrication of Microfluidic and Optofluidic molds with SPE-60 Photoresist: Advantages and Challenges

Sajjad Aghajari, Mohammadmehdi Jahanbakhshian, and Rouhollah Karimzade*

Department of Physics, Shahid Beheshti University, Tehran, Iran

*Corresponding author email: r_karimzade@sbu.ac.ir

Received: Sept. 30, 2023, Revised: Feb. 02, 2024, Accepted: Feb. 04, 2024, Available Online: Feb. 06, 2024
DOI: 10.61186/ijop.17.1.65

ABSTRACT— One of the basic requirements in the fabrication of microfluidic (MF) and optofluidic (OF) chips is a suitable initial mold, which is generally prepared with the help of a photoresist material. In this research, we investigate the SPE-60 photoresist as a quality alternative to the conventional SU-8 photoresist to achieve molds with thicknesses ranging from 25 μ m to 130 μ m and address the challenges of mold-making with this photoresist. The conventional photolithography method is used to assess the material's ability in mold making. The results show that SPE-60 molds have vertical edges, clean facets, and edges, complete voids between different components, and demonstrate good pattern transfer from the photomask to the SPE-60 film at various thicknesses. This article also suggests some ways to improve accuracy and reduce edge scattering. As a result, based on the experimental results, SPE-60 can be considered a cost-effective and suitable alternative to SU-8 photoresist in the fabrication of MF and OF molds.

KEYWORDS: Microfluidic, Mold, Optofluidic, Photolithography, Photoresist, SPE-60, SU-8

I. INTRODUCTION

The late 20th century saw the emergence of microfluidic chips (MF) [1], which originated from the photolithography process that enabled microelectronics and integrated circuits (IC) in 1955 [2], [3]. MF is the science and technology of systems that confine fluids to microscale dimensions within a small and integrated structure and study and analyze their behavior [4], [5]. Typically, “small” means volumes less than a milliliter [6], [7], in

channels with sub-millimeter scale dimensions [8], [9]. An MF chip has one or more inputs/outputs that connect with the macroscale world [7].

Using microelectromechanical systems (MEMS) technology, optofluidic chips (OF) integrate optical components into microfluidic chips [10], [11], creating truly portable and low-volume microsystems [12], [13].

MF/OF chips can be produced either through direct fabrication or replication [9]. Replication involves using a template with microfeatures, which is then molded to create copies [14]. This method can significantly reduce fabrication costs if it is repeatable [15]. The microstructures are created from the molds, and the products are duplicated from them [16]. After the initial prototyping, the mold can be used stably, even though the process of creating high-resolution molds may be slow [4].

A method for creating flat molds is photolithography [17]. It involves coating a substrate with a light-sensitive material, known as photoresist, and exposing it to light, which shields the desired areas from subsequent processes like etching or deposition. The light passes through a photomask with the two-dimensional pattern of the features. The mask is positioned between the light source and the coated substrate. Subsequently, methods can be used to separate the materials from the substrate [18].

Optofluidic (OF) chips made from photolithography molds have smooth surfaces in the fluid channels and the light-shaping components, which reduce light attenuation and transmission losses [12]. This makes them superior to other mold-making methods or direct chip fabrication.

The photoresist can be either negative or positive [16], depending on whether it remains or dissolves after light exposure [7]. SU-8 is a negative epoxy-based photoresist known for its high resolution, mold durability, and high aspect ratio, making it suitable for MF/OF molds [15]. Photolithography of SU-8 employs ultraviolet light with wavelengths ranging from 320nm to 450nm [9].

SU-8 has low thermal conductivity, which can limit its applications in high-power or heat-dissipation devices [19]. It also possesses a high thermal expansion coefficient, which can induce significant internal stress, potentially resulting in cracking or delamination of the film and affecting the mechanical and electrical performance of the chip [20]. Moreover, it exhibits poor adhesion to substrates such as glass, which may lead to the SU-8 film peeling off during processing [21]. Furthermore, SU-8 is sensitive to moisture and oxygen, which can degrade its chemical and physical properties over time [22].

Considering the challenges associated with SU-8 and the cost reduction goals of chip-based devices, SPE-60 was selected as a suitable photoresist for MF/OF molds. SPE-60 finds utility in the electronics industry for applications such as printed circuit boards, flexible printed circuits, touch panels, and more. It is also employed in electronic devices requiring fine patterns and high reliability, as well as in the automotive and telecommunications sectors.

Table 1 presents some features of SPE-60 photoresist. SPE-60, a negative photoresist, boasts high resolution, alkali-degradability, and high acid resistance. Additionally, it exhibits lower viscosity, facilitating easier and more uniform spinning or spreading. It can be

removed with a weak alkali solution in a short time, in contrast to SU-8, which necessitates stronger solvents like N-methyl-pyrrolidone (NMP) or propylene carbonate (PC) at higher temperatures and longer durations, potentially causing substrate damage. Furthermore, SPE-60 can be stored for six months at 20°C in a dark place without any loss of quality.

This work explores the optimal photolithography parameters for SPE-60 photoresist in the fabrication of MF/OF molds with thicknesses ranging from 25 to 130 microns. Typically, SPE-60 is primarily employed for thicknesses below 50 micrometers in the electronics industry.

Table 1. Key features of SPE-60 photoresist.

Features	Description
Viscosity	40-100 PS at 25°C
Pencil hardness	$\geq 2H$
Shelf life	6 months at 20°C in a dark place
Resolution	15-25 microns
Photo Exposure	30-100mJ/cm ²
Developer	5wt% NaOH at 50°C in 30-60s

II. MATERIAL AND METHOD

In contrast to the typical molds used for MF/OF applications, which employ SU-8 photoresist for photolithography, SPE-60, a photo-imageable resist ink, was obtained from Seoul Chemical Research Laboratory Co., Ltd. The wavelength absorption of SPE-60 is illustrated by its UV-visible spectrum in Fig. 1. Glass slides serve as the substrate for mold fabrication. These glass slides possess a refractive index of 1.56 and a surface roughness of less than 2nm, rendering them suitable for mold production as they minimize scattering during optical performance. The following paragraphs elucidate the process of forming the SPE-60 mold on glass substrates.

Figure 2 illustrates the steps involved in the photolithography process. To clean the substrate's surface, it is first washed with soap and water, then immersed in a beaker containing acetone and subjected to ultrasonic cleaning for 180 seconds. This step removes any organic material that might interfere with mold formation. Subsequently, the glass slide

is baked at 90°C for 10 minutes to eliminate all water molecules from the glass surface, as water can disrupt the mold formation process.

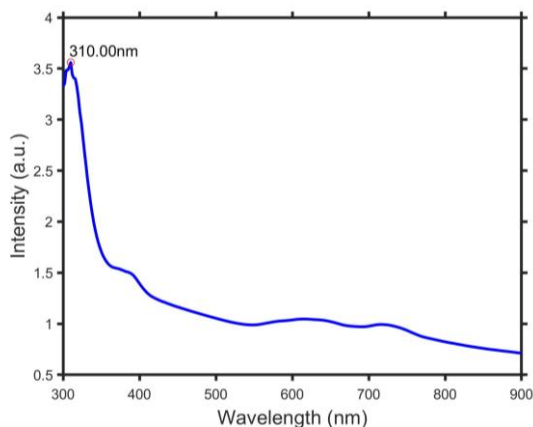


Fig. 1. The absorption peak of SPE-60 photoresist at wavelength 310nm.

The cleaned and contamination-free glass slide is then placed on a spin coater device, and a quantity of SPE-60 is poured onto it, creating a uniform layer through rotation. The thickness of this film is controlled by adjusting the time and speed of the spin coater. The coated substrate undergoes a soft-bake process at an appropriate temperature and time. This step serves to evaporate the solvents present in the photoresist, with the baking time varying depending on the thickness. It's important to note that high temperatures are avoided in this step to prevent thermal issues. Once the coated substrate has cooled to room temperature, a photomask with the desired pattern is placed on the film and exposed to light.

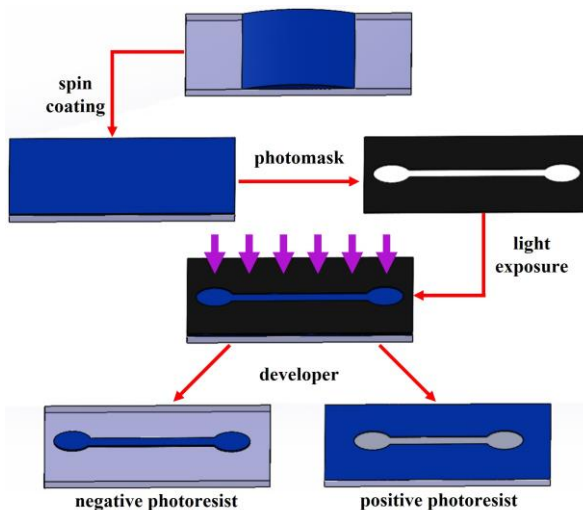


Fig. 2. Photolithography process.

The LED light is employed to expose and transmit the pattern onto the film. The spectrum of the light source used is depicted in Fig. 3. Subsequently, the exposed film is positioned on a hot plate for a post-bake process, conducted at an appropriate temperature and duration. After this step, the mask image becomes visible on the SPE-60 film. Because it is a negative photoresist, the exposed areas solidify and persist after immersion in the developer solution. Ultimately, the residual pattern of the photoresist serves as the mold for crafting chip-based devices.

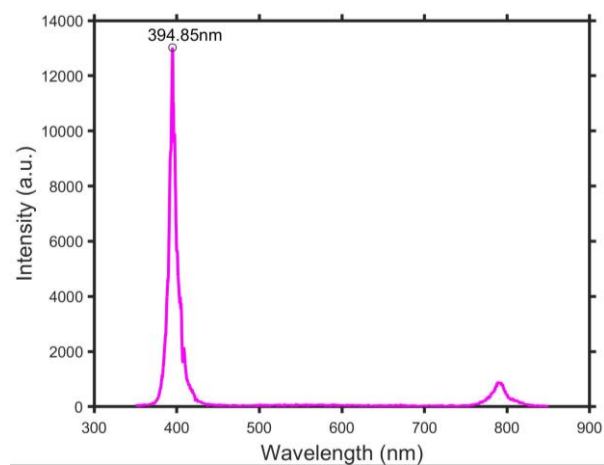


Fig. 3. Spectrum of the light source with wavelength 394.85nm.

The photolithography process for SPE-60 is carried out in a darkroom with a light source exhibiting the spectrum depicted in Fig. 4. This is essential because other wavelengths can adversely affect SPE-60 and impede pattern transfer or development.

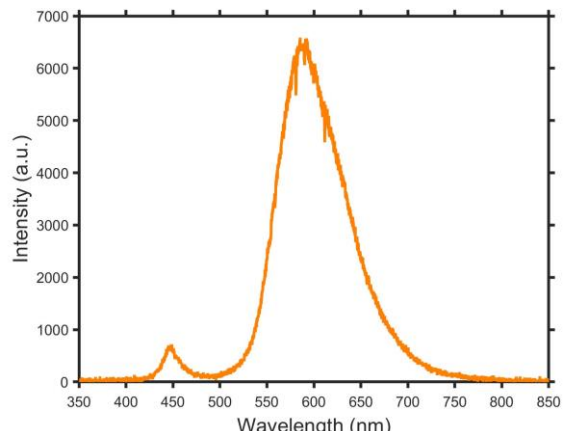


Fig. 4. Spectrum of the light source in a darkroom setting.

III. EXPERIMENTAL RESULTS

In this section, we scrutinize the experimental data for each step of the photolithography process and its associated parameters. We investigated three parameters of the spin coating device: total spin time, spin speed, and time to reach maximum speed. After conducting multiple tests while keeping the values of total spin time (50 seconds) and time to reach maximum speed (20 seconds) consistent for different thicknesses, these settings were selected and maintained for all subsequent experiments. The thickness measurements were reported with an accuracy of “ $\pm 10\mu\text{m}$,” as shown in Table 2.

To examine the impact of spin speed on film thickness, several tests were conducted, and the results are presented in row 1 of Table 2. As anticipated, increasing the speed reduced the film thickness on the substrate, leading to improved uniformity in material distribution. Following the application of the photoresist onto the substrate, a slow baking process was necessary to evaporate the solvent and thicken the layer. It is advisable to use a heat source with precise and uniform temperature control for soft baking. By conducting tests at various temperatures, we determined that 130°C was the optimal and constant temperature for soft baking. Lower temperatures resulted in incomplete solvent removal or extended removal time for the photoresist, while higher temperatures caused the material bonds to become so strong that they hindered the transfer of the photomask pattern during exposure.

Subsequently, efforts were made to determine an appropriate baking time for each thickness, as illustrated in row 2 of Table 2, revealing a threefold increase in baking time for minimum and maximum thicknesses. After the soft baking process, the coated substrate was allowed to cool down to room temperature by leaving it in the environment for 10 minutes.

Subsequently, the carefully designed photomask is placed onto the coated substrate and exposed to light. Two crucial parameters in this phase are the contact between the mask

and the film and the intensity of the light. To achieve smooth and uniform edges with high resolution, it is essential to establish maximum contact between the photomask and the film. However, since photomasks are dark and transparent surfaces, the boundary between the two surfaces can cause edge scattering. In areas where distances between components are small and details are critical, the intensity of the light becomes a significant factor.

Increasing the light intensity results in a faster reaction of the film to light and expedites the pattern transfer process. However, it also increases edge scattering, particularly noticeable with increasing thickness. This can lead to a loss of smoothness and sharpness in the edges. If the edges are not smooth, scattering occurs from the surfaces, impacting the performance of optical components, which rely on having well-defined patterns. During the exposure step, 20 watts of power from the light source were utilized for patterns with $100\mu\text{m}$ distances.

The data about exposure times for different thicknesses are documented in row 3 of Table 2, revealing a significant increase in exposure time as the film thickness grows, ranging from minutes to hours. Following exposure, the film undergoes the post-bake process, after which the photomask image becomes visible on the photoresist film. In rows 4 and 5 of Table 2, the results of experiments for determining the optimal temperature and duration for the post-bake process are presented. These findings affirm that achieving the desired outcome necessitates both more time and higher temperatures for thicker layers. Any shortcomings in achieving a clear transfer of the mask pattern can be attributed to defects occurring during the soft-bake or light exposure stages.

Subsequently, the film is allowed to cool at room temperature for 5 minutes. This step promotes the cross-linking of SPE-60 molecules and forms the required hard structures. Both the exposure step and this cooling step play crucial roles in determining the final mold's quality, significantly

impacting the presence of excessive cracks and resolution. It is imperative to optimize these two steps. In the developer step, a chemical bath comprising NaOH and distilled water with a concentration of 5mg/ml is prepared.

Table 2. Data related to SPE-60 photolithography experiment.

Thickness (μm)	25	35	45	65	95	130
Spin speed (rpm/min)	3000	2500	2000	1500	1000	800
Soft-bake time (min)	10	15	15	15	20	30
Light exposure time (s)	60	100	220	1000	4500	16000
Post-bake temperature (°C)	2	3	3	4	4	5
Post-bake time (min)	100	100	100	100	130	130
Developer time (min)	2	3	3	4	4	5

After evaluating various parameters for SPE-60, the potential to produce high-quality molds for MF/OF chips was established, enabling them to compete with SU-8. Mold resolution is a critical aspect of quality control in mold production. This encompasses ensuring the accurate transfer of patterns onto the mold and the precise formation of all features, minimizing small defects that could impact the mold's performance. These defects may involve issues like cracking, pattern transfer accuracy, and cleanliness.

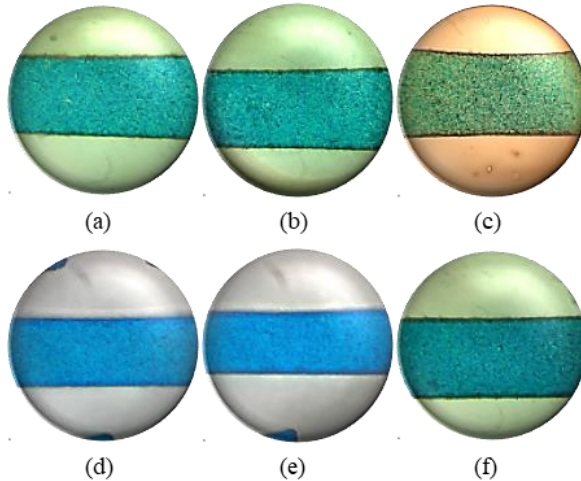


Fig. 5. Images of SPE-60 molds with different thicknesses. (a) 25μm, (b) 35μm, (c) 45μm, (d) 65μm, (e) 95μm, (f) 130μm.

Figure 5 displays images depicting the smoothness and uniformity of surfaces created by SPE-60 molds at various thicknesses. Ensuring the precise formation of angles, channels, grooves, and micro-lenses is a critical concern in MF/OF chips, as illustrated in Fig. 6. In both Figure 5 and Figure 6, the molds exhibit vertical edges, high resolution,

Immersion times were varied as parameters in the experiments, and the results are recorded in row 6 of Table 2. Following this, the surface is rinsed with distilled water and then dried in an oven at 60°C for 10 minutes.

Table 2. Data related to SPE-60 photolithography experiment.

clean facets, sharp edges, voids completely devoid of materials, and successful pattern transfer from the mask to the substrate across different thicknesses.

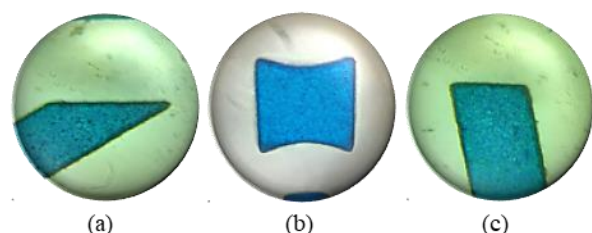


Fig. 6. Demonstrating SPE-60's capability in molding sharp angles and complex designs with varied thicknesses. (a) 95μm, (b) 130μm, (c) 95μm.

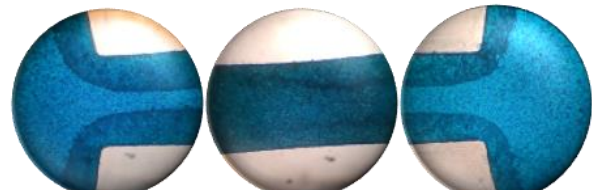


Fig. 7. Visual representation of non-uniformity in various areas of the SPE-60 mold resulting from insufficient exposure time.

Various components of a mold with a thickness of 50μm are observed in Fig. 7, highlighting surface non-uniformity. To examine the surface's thickness uniformity, the mold underwent a Dektak profilometer, the results of which are presented in Fig. 8, revealing consistent thickness across the mold surface. However, it was discerned that the surface non-uniformity, despite the surface's consistent thickness, could be attributed to the brief duration of light irradiation and the elongated reaction time of SPE-60 with increasing thickness. In essence, the darker

areas correspond to regions where the chemical reaction has not fully occurred, and the photoresist has not fully hardened. These areas require more time to establish the reaction and undergo polymerization.

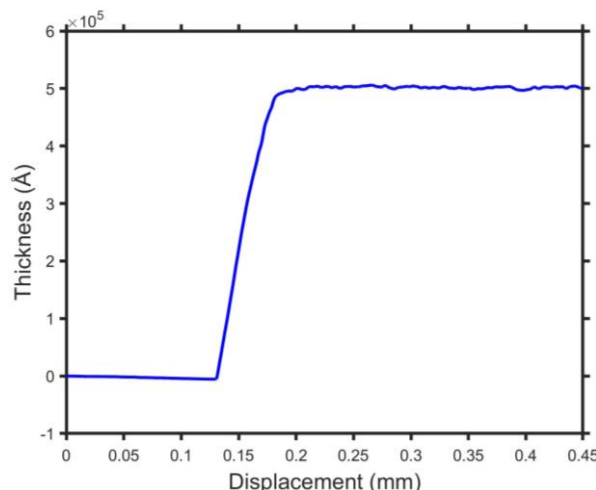


Fig. 8. The profile of the fabricated pattern measured by Dektak profilometer.

The precise transfer of the pattern onto the film through exposure requires careful attention. As previously mentioned, the contact between the film and the photomask holds significant importance. During the fabrication process, it was observed that when the photomask establishes good contact with the film, the molds exhibit excellent clarity. Conversely, when contact is inadequate in certain areas, the clarity of the pattern transfer becomes markedly poor. Figure 9 illustrates such a mold where it is evident that not all the material has been removed due to an incomplete pattern transfer. This incomplete transfer can lead to noticeable damage in mold performance, particularly for micro-lenses with varying curvature and lower surface quality.

The issue of poor pattern transfer is primarily attributed to weak contact, resulting in light scattering and exposing areas that should remain dark, and vice versa. This leads to the creation of areas that have been partially exposed, with low interfacial bond strength, making complete cleaning challenging.

The proper fabrication of molds is paramount for ensuring the efficient and optimal

performance of MF/OF chips. Consequently, this research conducted a thorough examination of mold quality to facilitate the effective formation of SPE-60 molds, with necessary adjustments made to the fabrication process to rectify issues associated with poor performance or low-quality molds. This study investigated the fabrication of high-quality molds for MF/OF chips using the photolithography method and SPE-60 photoresist. Various parameters, including spin speed, soft-bake temperature and duration, exposure intensity and time, post-bake temperature and time, and developer time, were systematically altered to assess their impact on mold thickness and clarity.

The findings revealed that increasing the spin speed resulted in a reduction in film thickness, with 130°C identified as the optimal soft-bake temperature. Moreover, elevating exposure intensity led to a decrease in exposure time but increased edge scattering in the pattern. The post-bake temperature and duration exhibited a direct relationship with film thickness. Additionally, the use of NaOH solvent rendered the pattern on the SPE-60 film visible.

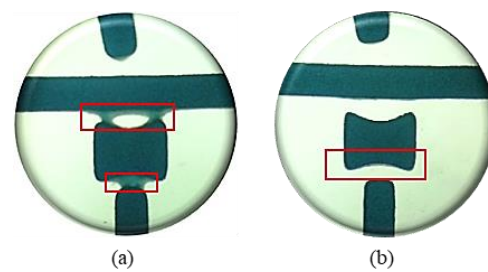


Fig. 9. The poor pattern transfer due to weak contact causes light diffraction. (a), (b) Poor transmission of the optical system from the photomask to the film that affects the performance of the mold.

In summary, the results demonstrated that SPE-60 molds possess vertical edges, clean facets, and sharp edges, along with complete voids between different components, facilitating excellent pattern transfer from the mask to the SPE-60 film across various thicknesses. Furthermore, SPE-60 molds proved capable of creating complex patterns with high precision on the SPE-60 film. However, further investigation is warranted to

explore the impact of other parameters, such as the type and shape of the mask, substrate properties, and more.

IV. CONCLUSION

In this study, experimental tests were conducted to explore the use of negative SPE-60 photoresist in the production of molds with varying thicknesses. Different parameters for mold fabrication through the photolithography method were optimized to accommodate these varying thicknesses. The quality of the molds, particularly for thicknesses below 100 μ m, stands out in comparison to SU-8. Furthermore, to enhance accuracy and reduce edge scattering, light sources with wavelengths close to SPE-60's absorption wavelength can be employed. Ultimately, SPE-60 can serve as a cost-effective and suitable alternative to conventional photoresists in the fabrication of MF/OF molds, marking a significant step in cost reduction for MF/OF chips.

REFERENCES

- [1] G. Zhu and N. Trung Nguyen, "Particle sorting in microfluidic systems," *Micro and Nanosystems*, Vol. 2, no. 3, pp. 202-216, 2010.
- [2] N. Convery and N. Gadegaard, "30 years of microfluidics," *Micro and Nano Engineering*, Vol. 2, pp. 76-91, 2019.
- [3] W.-C. Tian and E. Finehout, *Introduction to microfluidics*, in *Microfluidics for biological applications*: Springer, pp. 1-34, 2008.
- [4] J. Tang, G. Qiu, and J. Wang, "Recent development of optofluidics for imaging and sensing applications," *Chemosensors*, Vol. 10, no. 1, pp. 1-20, 2022.
- [5] Y. Zhang, B. R. Watts, T. Guo, Z. Zhang, C. Xu, and Q. Fang, "Optofluidic device based microflow cytometers for particle/cell detection: a review," *Micromachines*, Vol. 7, no. 4, pp. 1-21, 2016.
- [6] P. Shivhare, A. Bhadra, P. Sajeesh, A. Prabhakar, and A. Sen, "Hydrodynamic focusing and inter distance control of particle-laden flow for microflow cytometry," *Microfluidics and Nanofluidics*, Vol. 20, pp. 1-14, 2016.
- [7] A. Burklund, A. Tadimety, Y. Nie, N. Hao, and J.X. Zhang, "Advances in diagnostic microfluidics," *Adv. Clin. Chem.*, Vol. 95, pp. 1-72, 2020.
- [8] R. Blue and D. Uttamchandani, "Recent advances in optical fiber devices for microfluidics integration," *Journal of Biophoton.*, Vol. 9, no. 1-2, pp. 13-25, 2016.
- [9] S.M. Scott and Z. Ali, "Fabrication methods for microfluidic devices: An overview," *Micromachines*, Vol. 12, no. 3, pp. 1-38, 2021.
- [10] Y. Zhao, Q. Li, X. Hu, and Y. Lo, "Microfluidic cytometers with integrated on-chip optical systems for red blood cell and platelet counting," *Biomicrofluidics*, Vol. 10, no. 6, pp. 064119(1-13), 2016.
- [11] Z. Shen, Y. Zou, and X. Chen, "Characterization of microdroplets using optofluidic signals," *Lab on a Chip*, Vol. 12, no. 19, pp. 3816-3820, 2012.
- [12] S. Hengoju, S. Wohlfel, A. S. Munser, S. Boehme, E. Beckert, O. Shvydkiv, M. Tovar, M. Roth, and M. A. Rosenbaum, "Optofluidic detection setup for multi-parametric analysis of microbiological samples in droplets," *Biomicrofluidics*, Vol. 14, no. 2, pp. 024109(1-12), 2020.
- [13] A. Mohan, P. Gupta, A. Nair, A. Prabhakar, and T. Saiyed, "A microfluidic flow analyzer with integrated lensed optical fibers," *Biomicrofluidics*, Vol. 14, no. 5, pp. 054104(1-16), 2020.
- [14] Y.-J. Juang and Y.-J. Chiu, "Fabrication of polymer microfluidics: An overview," *Polymers*, Vol. 14, no. 10, pp. 2028(1-18), 2022.
- [15] B.K. Gale, A.R. Jafek, C.J. Lambert, B.L. Goenner, H. Moghimifam, U.C. Nze, and S.K. KamarapuI, "A review of current methods in microfluidic device fabrication and future commercialization prospects," *Inventions*, Vol. 3, no. 3, pp. 1-25, 2018.
- [16] A. Alrifaiy, O.A. Lindahl, and K. Ramser, "Polymer-based microfluidic devices for pharmacy, biology, and tissue engineering," *Polymers*, Vol. 4, no. 3, pp. 1349-1398, 2012.
- [17] M.A. Lake, C.E. Narciso, K.R. Cowdrick, T.J. Storey, S. Zhang, J.J. Zartman, and D.J. Hoelzle, "Microfluidic device design, fabrication, and testing protocols," 2015.

[18] V. Cardoso and G. Minas, *Micro total analysis systems, Microfluidics and Nanofluid. Handbook: Fabrication, Implementation and Applications*; CPTF Group, Ed, pp. 319-366, 2011.

[19] W. Zhou, Y. Li, Y. Sun, J. Yao, X. Song, and G. Ding, "Enhancement of Mechanical and Thermal Properties of SU-8 Photoresist with Multilayer Woven Glass Fabric Based on Micromachining Technology," *Electron. Materials Lett.*, Vol. 16, pp. 604-614, 2020.

[20] M.D. Gupta, R.B. Mishra, I. Kuriakose, and A.M. Hussain, "Determination of thermal and mechanical properties of SU-8 using electrothermal actuators," *MRS Adv.*, Vol. 7, no. 28, pp. 591-595, 2022.

[21] J. Liu, D. Song, G. Zong, P. Yin, X. Zhang, Z. Xu, L. Du, C. Liu, and L. Wang, "Fabrication of SU-8 moulds on glass substrates by using a common thin negative photoresist as an adhesive layer," *J. Micromech. Microeng.*, Vol. 24, no. 3, p. 035009(1-5), 2014.

[22] F. Ceyssens and R. Puers, *SU-8 Photoresist*," in *Encyclopedia of Nanotechnology*, B. Bhushan Ed. Dordrecht: Springer Netherlands, pp. 2530-2543, 2012.



Sajjad Aghajari was born in Ahvaz, Iran, in 2000. He received his BSc degree in physics from Shahid Chamran University, Ahvaz, Iran in 2021. He is currently a MSc student in optics and laser physics at Shahid Beheshti University, Tehran, Iran. His research interests include optofluidic devices, photonic integrated, and fiber optics sensors.



Mohammadmehdi Jahanbakhshian was born in Kerman, Iran, in 1989. He received his BSc degree in physics from Shahid Bahonar University, Kerman, Iran, in 2012, MSc degree in atomic and molecular physics and PhD degree in optics and laser physics from Shahid Beheshti University, Tehran, Iran, in 2014 and 2022, respectively. He is currently a research assistant at Shahid Beheshti University. His research interests include fluorescence microscopy, programming, and fiber optics sensors.



Rouhollah Karimzadeh received his BSc degree in Physics from Tabriz University, Tabriz, Iran, in 2003, and the MSc degree in Physics from Shahid Beheshti University, Tehran, Iran, in 2005. He obtained his PhD degree in Physics from Shahid Beheshti University, Tehran, Iran, in 2011. From 2011 to 2016, he served as an assistant professor at Shahid Beheshti University. Since 2016, he has been an associate professor at the same institution. His research interests include the interaction of light and matter, nonlinear optics, optofluidics, and microfabrication.